Food Hydrocolloids 173 (2026) 112242

Contents lists available at ScienceDirect

Food Hydrocolloids

journal homepage: www.elsevier.com/locate/foodhyd

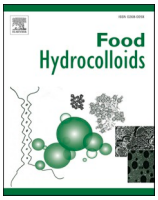

Effect of heat treatment on casein micelle structure and acid and rennet gel properties in goat and cow milk – a SESANS approach

Swantje Breunig [a,b,1], Zekun Fan [a,*,1], Renske Bouma [a], Gregory N. Smith [c], Rafael V.M. Freire [d], Ilja K. Voets [d], Steven R. Parnell [c,e], Kasper Hettinga [a], Etske Bijl [a]

[a] Food Quality and Design Group, Wageningen University and Research, Wageningen, the Netherlands
[b] Ausnutria B.V., Zwolle, the Netherlands
[c] ISIS Neutron and Muon Source, Rutherford Appleton Laboratory, Didcot, OX11 0QX, United Kingdom
[d] Laboratory of Self-Organizing Soft Matter, Department of Chemical Engineering and Chemistry and Institute for Complex Molecular Systems, Eindhoven University of Technology, Eindhoven, the Netherlands
[e] Faculty of Applied Sciences, Delft University of Technology, Delft, the Netherlands

ARTICLE INFO

Keywords:
Acid gels
Rennet gels
Casein
Goat milk
Cow milk
Spin-echo small-angle neutron scattering

ABSTRACT

Acid and rennet gelation are essential processing steps for dairy products such as cheese and yoghurt. The coagulation and gel properties of these gels differ depending on whether unheated or heated milk was used. However, these heat-induced effects occur to a different extent in goat and cow milk gels, and have yet to be determined on a micro- and nanoscale structural level. To obtain a better understanding of heat-induced structural changes, this study investigates non-heated and heated casein micelle solutions from goat and cow milk and their derived rennet and acid-induced gels by a multi-technique approach, combining rheology, confocal scanning laser microscopy, and spin-echo small-angle neutron scattering (SESANS). This work is thereby the first to describe heat-induced changes of caseins and casein gels using SESANS. Modeling casein micelles as sticky hard spheres shows that goat caseins are larger and less hydrated than their cow counterparts. SESANS data reveal that structural changes observed in rennet and acid gels follow opposite trends when milk was pre-heated. Modeling gels as fractal gels suggests a connection between heat treatment and changes in the arrangement of caseins to form more loose or compact aggregates. Cow milk gels showed larger heat-induced changes in SESANS and corresponding larger rheological changes than goat milk counterparts. This work shows that rennet and acid gels respond differently to pre-heat treatment, and that they differ in the compactness of their casein network. The findings from this study can contribute to the design and characterization of dairy products of different animal species.

1. Introduction

Cow milk is the main source of dairy worldwide and hence also the most studied milk type. But with the increasing demand for goat milk products, the goat milk industry is facing technological challenges in manufacturing goat milk products (Akshit et al., 2024; de Asís Ruiz Morales et al., 2019; Miller & Lu, 2019). Therefore, there is also an increasing need to understand these challenges and differences between products manufactured from cow and goat milk.

For many dairy products made from cow and goat milk, gelation is a common processing step in the dairy industry. Milk gel formation is typically caused by aggregation of the main protein fraction, the casein (CN), into a space-spanning network. In milk, individual casein proteins associate with each other, forming spherical colloidal structures called casein micelles. These casein micelles are stabilized against aggregation at the natural pH of milk by electrostatic and steric interactions (Horne, 2020). Both goat and cow casein consist of four casein fractions: κ-CN, α_{S2}-CN, α_{S1}-CN, and β-CN. However, the overall casein composition differs between goat and cow milk; β-CN is the main casein fraction in goat milk, whereas cow milk contains equal levels of α_{S1}-CN and β-CN (Breunig, Gonzalez-Prendes, et al., 2025; Park, 2017). Upon acidification or enzymatic cleavage, casein micelles lose their repulsive forces

* Corresponding author.
E-mail address: zekun.fan@wur.nl (Z. Fan).
[1] Joint first authorship.

https://doi.org/10.1016/j.foodhyd.2025.112242
Received 4 August 2025; Received in revised form 27 October 2025; Accepted 10 November 2025
Available online 11 November 2025

that are essential for their stabilization, which causes them to aggregate (Horne, 2020). However, it is important to realize that their aggregation mechanisms differ: Acid gelation is mainly a result of particle charge neutralization, whereas rennet gel formation occurs due to the cleavage of κ-CN, removing repulsive forces of the casein micelle (Lucey, 2020). Both gel types, though, are classified as particle gels, as casein micelles also retain most of their micellar structure during gelation to a large extent (Bremer et al., 1989; Horne, 1999; Lucey, 2020). To better describe milk gel properties, milk gel structure has been described using a fractal model (Bremer et al., 1989; Lucey & Singh, 1998; Yang et al., 2023). In fractal systems, building blocks (e.g., casein micelles) aggregate in a fractal manner, forming self-similar patterns across multiple length scales.

The properties of milk gels, such as gel strength, are not only determined by processing steps, such as heating, acidification, and renneting, but are also determined by the milk source. For instance, acid gels made from unheated cow milk form stronger gels than when formed from unheated goat milk (Li et al., 2023; Roy, Ye, Moughan, & Singh, 2020). The reason for this is not understood, but could be linked to differences in the casein composition. In addition to the animal origin of milk, pre-heating of milk, which is necessary to ensure microbial safety of dairy products, has a significant effect on gel formation. Heat treatment of milk causes the whey proteins in milk to unfold and aggregate. A considerable fraction of whey proteins thereby associates with the casein micelles in milk, altering their gel formation abilities (Donato & Guyomarc'h, 2009; Li et al., 2022; Lucey et al., 1998). Acid gel formation is improved by pre-heating of milk, whereas rennet gelation is impaired. This phenomenon is observed in both goat and cow milk, but to different extents (Breunig, Fan, et al., 2025; Li et al., 2023). The reasons behind this are not yet fully understood. The changes of gel strength and coagulation time with pre-heating of milk have been widely described in the literature, especially for cow milk. However, describing the structural differences of milk gels made from different milk sources or comparing milk gels from unheated and heated milk at a structural level is difficult, primarily because food structures such as milk gels cover a wide range of length scales. Nevertheless, understanding structural differences of milk gels could provide valuable insights and improve the elucidation of gelling differences among milks from different animals and under heat treatments.

Structural information can be obtained using small-angle neutron scattering (SANS) techniques, which have proven to be powerful techniques for studying casein micelles and milk gel structure (Gilbert, 2019; Smith, 2021; Van Heijkamp et al., 2010). In addition to regular SANS, SESANS is a technique that measures bulk materials by using the Larmor precession of polarized neutrons to label the scattering angle. It can quantify neutrons to far smaller scattering angles, allowing measurements of structures of larger length scales than regular SANS (1–300 nm), covering length scales from ~30 nm up to 20 μm (Bouwman, 2021). It thereby presents a suitable technique to study food structures at the interface of nano and micro scales, such as milk gels. Examples of extractable sample properties include the size and arrangement of protein clusters and the sample's heterogeneities (Andersson et al., 2008; Bouwman et al., 2004; Rekveldt, 1996; Tromp & Bouwman, 2007). Compared to USANS, which probes similar length scales, SESANS provides results in real space, making data interpretation more intuitive than the reciprocal space data from USANS. In addition, SESANS is more tolerant to high concentrations and multiple-scattering than USANS, and it does not require the extreme slit collimation needed for USANS to probe very large scales and its consequent intense loss of flux. This can make SESANS potentially faster than USANS measurements (Bouwman, 2021).

There are rare examples of SESANS being applied to cow milk gels (mainly acid-induced gels) (Nieuwland et al., 2015; Van Heijkamp et al., 2010), however, no reports on either goat milk or goat milk gels. Furthermore, information on structural changes when heated milk was used is lacking. Previous works on milk gels using SANS or USANS focused on unheated samples and/or reconstituted samples (Callaghan-Patrachar et al., 2021; Nieuwland et al., 2015; Yang et al., 2023), were the first to study the effects of heating on acid gels using USANS (ultra-small-angle neutron scattering) and found increases in the fractal dimension and correlation length compared to gels from unheated milk, but the effect of heat treatment on rennet gels was not investigated.

In this work, we use SESANS to study casein micelles and the structure of acid and rennet-induced milk gels from heated and unheated goat and cow milk. SESANS data of casein micelles were modeled as sticky hard spheres (Smith, 2021; Smith et al., 2020), while scattering data of the gels was modeled using a fractal model (Bremer et al., 1989; Yang et al., 2023). The results are discussed and connected to rheological data, dynamic light scattering, and microscopy images. As both the structure and the functionality of casein micelles can be affected by sample pretreatment, properties of reconstituted milk and gels thereof may differ. Therefore, another highlight of this study is the preparation of native casein micelle solutions using a mild membrane filtration, which allows studying casein micelles and their gels with minimal impact from sample pretreatment. This work aims to provide novel insights into the structure of rennet and acid gels and how they are affected upon heating of milk. This could facilitate the rational design of dairy foods with optimal properties.

2. Materials and methods

2.1. Milk collection and preparation

Tank milk was collected from a local goat and cow farm in the Netherlands on the same day. Skim milk (SM) was prepared by centrifugation (3000×*g*, 20 °C, 30 min) and preserved with 0.02 % sodium azide and 1.65 mg/1000 g aprotinin. Heated skim milk (HSM) samples were prepared by heating SM for 30 min at 85 °C in a shaking water bath and subsequently cooled to room temperature on ice.

2.2. Preparation of casein micelle solution

Casein micelle solutions were prepared from non-heated and heated goat and cow SM by microfiltration followed by diafiltration using a Vivaflow 50 1,000,000 MWCO PES crossflow cassette (Sartorius AG, Germany). First, 150 mL skim milk was 3x concentrated with a speed of 300 mL/min at 50 °C. The concentrated milk was subsequently diafiltrated with 4x the volume of simulated milk ultrafiltrate (SMUF) prepared in D_2O (Jenness & Koops, 1962), which was preserved with 0.02 % sodium azide and 1.65 mg/1000 g aprotinin. The replacement of H_2O by D_2O in the samples is important to provide much better contrast and a cleaner background in neutron scattering measurements. As goat and cow milk have a comparable salt content and distribution (Breunig et al., 2024), the same SMUF was used for both milk types. After diafiltration, the volume of the diafiltrated milk was reconstituted to approximately 90 % of the original volume. This procedure allows the removal of soluble serum proteins (e.g., native whey proteins) as well as possible heat-induced soluble casein-whey protein aggregates while retaining micellar-bound proteins. Casein micelle solutions prepared from non-heated milk (NCM) and heated milk (HCM) were stored at 4 °C until further use.

2.3. Sample characterization

To ensure a similar protein content of all samples, the protein content of the initial NCM and HCM samples was analyzed by the DUMAS method (6.38 x total nitrogen) (Flash EA 1112 Protein analyzer, Thermo Fisher Scientific, Massachusetts, USA). Based on this, the samples were adjusted with SMUF to a protein content of 2.6 %, which is representative for the casein content in goat and cow milk. The samples were ultracentrifuged at 100,000×*g* for 1 h at 20 °C to determine the dry

matter content and volume fraction in duplicates. The dry matter of casein was determined after drying the casein pellet at 105 °C overnight.

2.4. Dynamic light scattering (DLS)

The z-average size of casein micelles in NCM and HCM was determined by dynamic light scattering (DLS). Samples were diluted 100 times in ultrapure (Milli-Q) water to minimize multiple scattering and subsequently filtered by using a 1.2 μm glass fiber membrane syringe filter (Phenomenex). Measurements were performed immediately after the filtration of skim milk by using a Zetasizer Ultra (Malvern Panalytical, UK). Samples were measured at 22 °C at a fixed scattering angle of 173° and a refractive index of 1.35 for the dispersant and 1.57 for the casein micelles. Two biological replicates were prepared, which were measured in triplicate, with 5 subruns per measurement (Breunig et al., 2024).

2.5. Protein composition characterization

The protein composition of the NCM and HCM samples was analyzed by reversed-phase high-performance liquid chromatography (RP-HPLC). Samples were prepared according to Breunig et al. (2024). Proteins were separated on a Discovery BIO Wide Pore C5 column (150 × 2.1 mm, 300 Å; Supelco, Sigma-Aldrich, St. Louis, MO) under elution conditions described by Breunig et al. (2024) for goat milk on a Widepore XB-C18 column (250 × 4.6 mm, 3.6 μm; Phenomenex, Utrecht, the Netherlands) and for cow milk under elution conditions based on Bonfatti et al. (2008). The chromatograms were analyzed with Chromeleon software (v.7.2.10; Thermo Scientific, Waltham, MA). The relative percentage of casein and whey was estimated by dividing the integrated peak area by the total integrated peak area of corresponding proteins.

2.6. Rheology

Rheological measurements were conducted with an Anton Paar 302 Rheometer (MCR 302e, Anton Paar GmbH, Austria), at 30 °C using a concentric cylinder. Rennet gels were prepared by adding 3.5 μL of freshly prepared 50x diluted CHY-MAX M 1000 chymosin (Chr. Hansen, Denmark) to 1.5 mL of sample. Acid gels were prepared by the addition of 1.5 % (w/v) glucono-δ-lactone (GDL). Subsequently, 1 mL of the sample was transferred to the measurement cups. Measurements were started at 2 min after sample preparation, at a frequency of 1 Hz and 1 % strain. Low viscous paraffin oil was added to the geometry to avoid water evaporation during measurements. Rennet gel formation was monitored over 6 h at 30 °C, and acid gelation over 16 h at 30 °C. In addition, the pH decrease during acid gelation was monitored.

2.7. Confocal laser scanning microscopy (CLSM)

The gel microstructure was assessed by CLSM. The measurements were carried out at the Wageningen Light Microscopy Center (WLMC) using a Leica Stellaris 5 confocal LSM (Leica, Germany). Samples were stained with 1 % v/v of 1 mg/mL of Fast green FCF in Mili-Q solution before gelling. Directly after rennet or GDL addition according to section 2.6, 300 μL sample was pipetted into a well of an 8-well μ-slide (Ibidi, Germany). The slide was closed and incubated as previously described. CLSM was performed at 640 nm (Bouma et al., 2025). Starting at 20 μm depth, 40 images were taken 0.25 μm apart in the z-direction, similar to Pax et al. (Pax, Ong, Kentish, & Gras, 2021).

2.8. Spin-echo small-angle neutron scattering (SESANS)

SESANS measurements were performed as single determinations on the LARMOR instrument at the ISIS Neutron and Muon Source (STFC Rutherford Appleton Laboratory, Didcot, U.K.) at 30 °C, as gelation was performed at this temperature. Liquid and gel samples were placed in a type 110 quartz cuvette with a sample path length of 2 mm (Hellma GmbH, Germany). For gel samples, samples were prepared according to section 2.6 and directly placed in a quartz cuvette after GDL and rennet addition and incubated at 30 °C in a water bath until loading the sample in the instrument. Gel samples were measured after 14–16 h of incubation for acid gels and after 6–8 h for rennet gels. Larmor was configured for SESANS operated at 1 MHz on the RF flippers and at poleshoe angles of either 84° (for fluids) or 55° (for gels). Different instrument settings make it possible to study different spin-echo lengths (δ), where δ is essentially the magnitude of the correlations being probed. The spin-echo length δ depends on the magnetic field strength, the angle between the magnetic field and the neutron beam (called the poleshoe angle), and the wavelength λ of the neutrons. The magnetic field strength was fixed for the 1 MHz configuration, and the neutron wavelength range used was $2.6 < \lambda < 11.95$ Å. The different poleshoe angles made it possible to probe different spin-echo lengths of either $44 < \delta < 920$ nm (for 84°) or $270 < \delta < 4000$ nm (for 55°). Data were processed by calculating the beam polarization on the detector as a function of neutron wavelength and then the normalized scattering correlation function calculated as a function of spin-echo length δ using bespoke Python algorithms implemented in the Mantid framework (Arnold et al., 2014). SESANS measurements determine the normalized scattering correlation function as a function of the spin-echo length δ by measuring the polarization of the neutron beam both with (P) and without (P_0) the sample. To obtain an instrument-independent scattering correlation function, the measured polarizations are normalized by the sample thickness t and the neutron wavelength λ to give the normalized scattering correlation function $(\ln(P/P_0)/(\lambda^2 t))$. A more detailed theoretical description of the SESANS technique can be found elsewhere (Andersson et al., 2008; Bouwman, 2021). Alongside these SESANS measurements, the transmission of the neutron beam was measured immediately after the sample position, both with and without the sample in the beam, to enable correction for lost scattering at the main (Li et al., 2019).

2.9. SESANS data analysis

The software SasView (v.6.0.0) was used to fit the SESANS data (https://www.sasview.org) (Bakker et al., 2020). The scattering from SANS is well described with equation (1):

$$I(q) = \frac{\phi}{V_b}(\rho_b - \rho_s)^2 P(q) S(q) + background \quad (1)$$

Where q is the magnitude of the scattering vector defined by $q = (4\pi/\lambda)\sin(\theta/2)$, λ being the neutron wavelength and θ being the scattering angle, and $I(q)$ is the scattering intensity as a function of q. ϕ is the volume fraction. The volume fraction of caseins (~0.1) was previously determined experimentally and fixed while fitting. V_b is the volume of a building block, ρ_b is the neutron scattering length density (SLD) of the casein micelle, and ρ_s is the neutron scattering length density of the solvent D_2O (6.38×10^{-6} Å^{-2}) (Smith, 2021). $P(q)$ and $S(q)$ are the form and structure factor associated with the shape and interparticle interactions, respectively. The built-in numerical Hankel transform feature from SasView was used to perform the conversion of the models calculated in reciprocal space to real space as measured in SESANS experiments (Andersson et al., 2008; Bakker et al., 2020).

2.9.1. Liquid samples

Casein micelles in liquid samples were modeled using the sticky hard sphere model in SasView (Smith, 2021; Smith et al., 2020). The casein micelles are modeled as polydisperse homogeneous spheres. The spherical form factor $P(q)$ depends on the radius r and is given as follows:

$$P(q) = \left[3V_b \frac{\sin(qr) - qR\cos(qr)}{(qr)^3}\right]^2 \quad (2)$$

The distribution of particle sizes was set as a log-normal distribution with its shape parameter $\sigma = 0.3$. The dimensionless structure factor $S(q)$ for casein micelles is obtained from the pair interaction potential $U(h)$:

$$U(h)/k_BT = \begin{cases} \infty \text{ for } h < 2r \\ \ln\left(\frac{12\tau\Delta}{\sigma+\Delta}\right) \text{ for } 2r < h < 2r+\Delta \\ 0 \text{ for } h > 2r+\Delta \end{cases} \quad (3)$$

Where h is the center-center separation, and τ is the (dimensionless) stickiness parameter associated with the adhesive strength. Contrary to the standard hard sphere model, in the sticky hard sphere model, there is a range of interparticle separations (Δ) in which the potential is neither 0 nor infinite (Baxter, 1968). Furthermore, for the structure factor $S(q)$, the so-called β-approximation was used to account for polydispersity and shape effects, which is an embedded function in SasView (Kotlarchyk & Chen, 1983).

2.9.2. Gelled samples

To describe the structure of gelled samples, the fractal model was used in this study to fit the data, following Teixeira (1998). This model describes the scattering from fractal-like aggregates of spherical particles.

$P(q)$ and $S(q)$ are the scattering from distributed particles (casein micelles) and the interference between particles associated in fractal-like aggregates. $P(q)$ can be calculated according to equation (2), $S(q)$ can be calculated as follows:

$$S(q) = 1 + \frac{d_f\Gamma(d_f-1)}{\left[1+\left(\frac{1}{q\,\xi}\right)^2\right]^{\frac{d_f-1}{2}}} \frac{\sin\left[(d_f-1)\tan^{-1}(q\,\xi)\right]}{(qR)^{d_f}} \quad (4)$$

Where ξ is the correlation length representing the average protein aggregate size, and d_f is the fractal dimension. During fitting, r was fixed based on the radius determined for casein micelles with the sticky hard sphere model. The polydispersity of micelle radii was described by a log-normal distribution with the σ parameter fixed to 0.3.

3. Results and discussion

3.1. Rheological characterization of deuterated milk gels

The gelation over time for rennet and acid gels made from goat and cow native (non-heated) (NCM) and heated (HCM) casein micelle solutions in D_2O were characterized. Fig. 1 shows the storage modulus G' over the gelation time. For NCM samples, goat NCM samples had a slightly higher maximum rennet gel strength G'_{max} (155.5 Pa) than cow NCM (150.0 Pa), whereas cow NCM (29.1 Pa) formed stronger acid gels than goat NCM (13.9 Pa). Differences in gel strength of unheated goat and cow milk are in agreement with earlier findings (Breunig, Fan, et al., 2025; Li et al., 2023). Upon pre-heating, the G'_{max} for HCM for acid gels increased compared to NCM for both goat and cow samples. That increase in G'_{max} was more pronounced in cow HCM. The opposite was the case for rennet gel samples; the G'_{max} showed a decrease for goat HCM compared to NCM. Cow HCM did not show gelation in contrast to goat HCM. The NCMs of both goat and cow milk prepared in D_2O thus exhibit similar changes in gel strength for acid and rennet gels upon heating compared to regular SM or casein micelles prepared in H_2O (Breunig, Fan, et al., 2025; Li et al., 2023), indicating that the results of this study using D_2O-based milk gels can be reasonably generalized to regular H_2O-based milk gels.

3.2. Characterization of casein micelles

3.2.1. Casein micelle composition and size (DLS)

The casein micelle radius determined by DLS, dry matter, volume

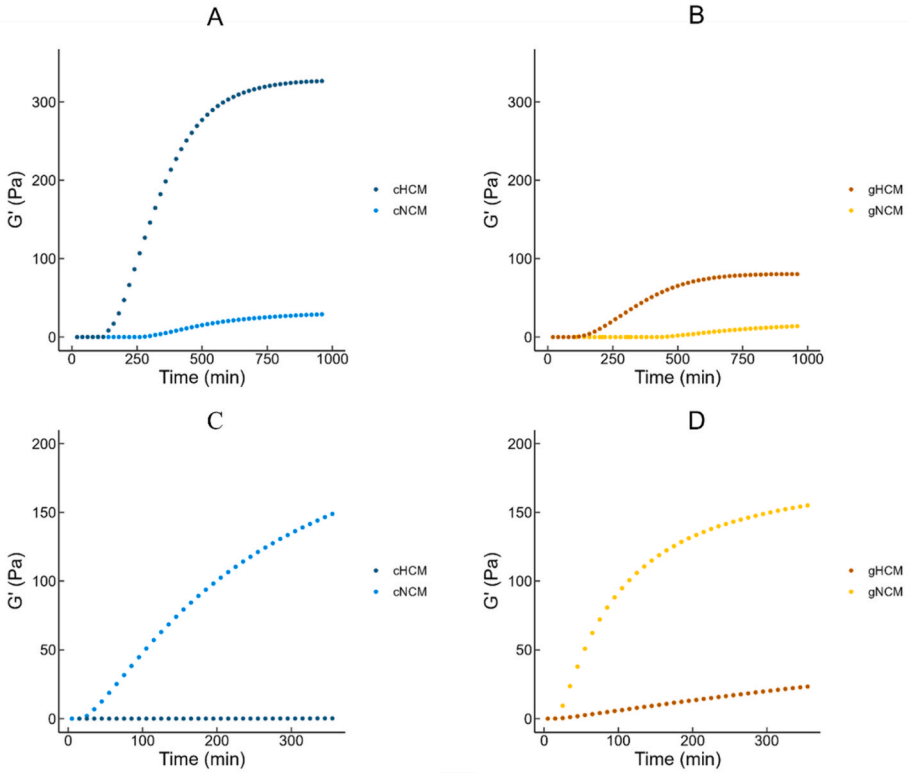

Fig. 1. Storage modulus (G') as a function of time for cow (A,C) and goat (B,D) native (NCM) and heated (HCM) casein samples for acid gelation (A,B) (1.5 % GDL, 30 °C, 16 h) and rennet gelation (C,D) (6 h 30 min).

fraction, as well as the protein composition for NCM and HCM of goat and cow milk are compared in Table 1. It shows that the overall casein composition of NCM and HCM is comparable to the casein composition in skim milk (Bijl et al., 2014; Breunig et al., 2024). Furthermore, as expected, goat NCM was larger than cow NCM (Ingham et al., 2018; Remeuf & Lenoir, 1986). The average casein micelle hydrodynamic radius for goat and cow HCM increased by about 5 nm compared to the corresponding NCM. Furthermore, HCM samples showed a lower casein: whey protein ratio compared to NCM, indicating that more whey proteins were present in the HCM samples. This is the case because whey proteins bind to casein micelles upon heating and are thus retained during the preparation of HCM samples.

3.2.2. Casein micelles as sticky hard spheres

SESANS data was used to further analyze the casein micelle structure. The SESANS data, as well as fitted curves for NCM and HCM samples, are shown in Fig. 2. Overall, the SESANS signal for both goat samples flattened at larger spin-echo lengths δ and showed higher signal strength (*i.e.,* more negative saturation level) than cow samples. This indicates a larger structure and/or a higher scattering length density contrast $\Delta\rho$ for goat NCM and HCM. To further compare the casein micelles and their changes upon heating, the SESANS data of liquid samples were modeled using the sticky hard sphere model. The fitting results for NCM and HCM from goat and cow milk are presented in Table 2. Results for the mean radius of cow NCM were in a similar range to that reported by Smith (2021), who used the same technique and model. The modeling results confirmed that the radius of goat NCM was larger than that of cow NCM, but differences in size were found to be larger in SESANS. The radii of casein micelles are thereby considerably smaller than detected by DLS (Table 1), especially for cow NCM and HCM. As DLS probes the intensity-weight hydrodynamic size of casein micelles (better accounting for the outer hairy layer), whereas SANS and SESANS are expected to rather measure the (protein-rich) core of casein micelles, differences in casein micelle size between these techniques can be expected (Fan et al., 2024; Tromp & Bouwman, 2007). After heat treatment, both goat and cow HCM showed an increase in radius, which can be explained by the fact that whey proteins covalently bind to casein micelles upon heating, thereby increasing the overall radius (Donato & Guyomarc'h, 2009).

Further differences were observed in the scattering length density contrast $\Delta\rho$ between the samples. Cow NCM and HCM showed lower $\Delta\rho$ compared to the goat equivalents, indicating a more hydrated structure for cow casein micelles. Comparing the dry matter of goat and cow milk, goat casein micelles indeed showed a higher dry matter content than cow casein micelles (Table 1), which is in line with Remeuf and Lenoir (1986). This difference in hydration could also contribute to the much larger divergences in micelle radius estimated between DLS and SESANS measurements for cow milk than for goat milk. The $\Delta\rho$ for both goat and cow HCM was higher than for their NCM equivalents. Even though changes in dry matter were not observed for goat and cow HCM compared to NCM in Table 1, the reduction in $\Delta\rho$ indicates an increase in hydration of HCM compared to NCM samples, which is expected upon heating (Gaucher et al., 2008). This increase in hydration (lowering in $\Delta\rho$) for HCM may also explain the lower signal strength for goat and cow HCM compared to NCM observed in Fig. 2. Using SESANS, differences in casein micelle size and hydration between goat and cow casein micelles were thus observed, as well as their changes that occur after heat treatment of milk.

Table 1
Characterization of native casein (NCM) and heated casein micelles (HCM) samples from cow and goat milk[a].

Parameter	cNCM	cHCM	gNCM	gHCM
Mean micelle radius (nm) (DLS)	77.85 ± 0.48	82.47 ± 1.20	86.79 ± 1.72	91.59 ± 1.37
Dry matter (%)	26.61 ± 0.19	26.96 ± 0.52	31.56 ± 0.21	31.36 ± 0.89
Volume fraction (%)	9.70 ± 0.12	8.96 ± 0.23	7.22 ± 0.35	7.52 ± 0.70
Casein composition (% of total corresponding casein)				
κ-CN	19.42 ± 0.14	17.01 ± 0.43	13.81 ± 0.35	12.30 ± 0.03
α_{S2}-CN	13.45 ± 0.10	14.00 ± 0.19	19.47 ± 0.51	19.20 ± 0.16
α_{S1}-CN	32.44 ± 0.24	32.56 ± 0.41	13.81 ± 0.35	12.30 ± 0.03
β-CN	34.69 ± 0.27	36.43 ± 0.21	52.25 ± 0.16	53.59 ± 0.06
Casein:whey ratio	0.95:0.05	0.89:0.11	0.94:0.06	0.89:0.11

[a] Parameters are reported as mean ± standard deviation.

3.3. Characterization of casein gels

3.3.1. Qualitative interpretation

The SESANS data for rennet and acid gels is shown in Fig. 3. Compared to the liquid samples, all rennet and acid gels showed a large increase in signal strength. The neutron signal flattens at larger spin-echo lengths δ than their corresponding liquid samples, indicating that structure formation at the micrometer scale occurred in all samples. Also the cow HCM rennet sample, which did not show gel formation in the rheological experiments, showed an increase in SESANS signal strength, as well as a curve that continued to decrease to larger length scales compared to liquid samples. This indicates that some structure formation also occurred in this sample (micelle aggregation). From the CLSM image (Fig. 4), it can also be observed that cow HCM formed aggregates upon rennet addition. These aggregates, however, did not form a continuous gel network but were still floating, which is why no (increase in) G' for cow HCM rennet gel was observed (Fig. 1).

From Fig. 3, further information can be obtained from the spin-echo length δ at which the SESANS signal of gels saturates. The SESANS signal for all gel samples saturates at around 2.5–3 μm. This number is related to the average size of the largest aggregates present in the sample and is in good agreement with the value of 3 μm observed with SESANS for yoghurt and curd by Tromp and Bouwman (2007). Furthermore, it can be observed that the maximum correlation length l_{max}, an indication of the largest structure present, for both goat and cow NCM rennet gels is larger than in acid gels, as the signal saturates at larger spin-echo length δ for rennet gels. Also, for HCM gels, the rennet gels showed a larger maximum correlation length l_{max}, but the difference compared to HCM acid gels was less pronounced than for gels formed from NCMs. Furthermore, changes in the signal strength could be observed depending on whether the gels were made from NCM or HCM. In both goat and cow rennet samples, the gels made from NCM have a higher signal strength than gels made from HCM, whereas the opposite was the case for the acid gels, for which the gels made from HCM showed a higher signal strength. This indicates that pre-heating of milk changes the gel structure in different ways depending on whether the gel is acid- or rennet-induced. This is in line with observations in section 3.1.

3.3.2. Casein gels as fractal structures

To obtain more quantitative results from the SESANS data, the gels were modeled with the fractal model. The results are presented in Table 3. Values for the correlation length ξ, which represent the average aggregate size in acid and rennet gels, range from 750 to 1000 nm, which is in good agreement with previously reported values on acid gels (Van Heijkamp et al., 2010; Yang et al., 2023). The correlation length ξ for acid gels was overall larger than for rennet gels, indicating that the average aggregates formed in acid gels were larger than in rennet gels. This contrasts to Tromp and Bouwman (2007), who indicated larger length scales in rennet-induced milk gels compared to the acid-induced milk gels. However, model-fitted values for rennet milk gels were not

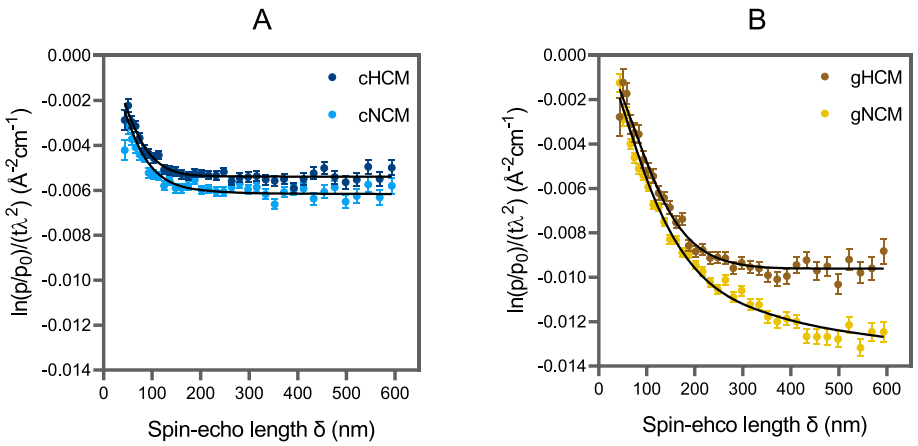

Fig. 2. SESANS signal as a function of spin-echo length (δ) for cow (A) and goat (B) native (NCM) and heated (HCM) casein micelle samples. Where P and P_0 are the polarization of neutron beams with and without passing the sample. t is the sample thickness and λ is the neutron wavelength. The solid black curves represent the fitted sticky hard sphere model.

Table 2
Results obtained from describing SESANS casein micelle structure for cow and goat native casein micelles (NCM) and heated casein micelles (HCM) with the sticky hard sphere model[a].

Parameter	cNCM	cHCM	gNCM	gHCM
Median sphere radius, r[b] (nm)	39.71 ± 3.29	44.89 ± 6.03	72.55 ± 1.95	92.63 ± 8.47
Log-normal distribution parameter, σ[c]	0.30	0.30	0.30	0.30
Volume fraction ϕ [c]	0.10	0.09	0.07	0.08
SLD difference, Δρ[b] (10^{-6} Å^{-2})	0.69 ± 0.02	0.60 ± 0.01	0.99 ± 0.01	0.90 ± 0.01
Stickiness parameter, τ[b]	0.11 ± 0.01	0.15 ± 0.07	0.09 ± 0.0	0.37 ± 0.68
Reduced χ-square, χ^2_R	0.89	0.88	1.67	1.60

[a] Parameters are reported as mean ± standard deviation.
[b] Fitted parameter.
[c] Fixed parameter.

reported earlier. Reasons for differences compared to Tromp and Bouwman (2007) could be the use of native casein micelles vs. reconstituted milk or differences in gel preparation. In addition, the amount of GDL added, for instance, can change the speed of acidification and may also affect gel formation (Jacob et al., 2011). No clear trend in correlation length ξ was observed for goat and cow rennet and acid gels when formed from HCM compared to NCM, indicating that heating prior to gelation did not change the average aggregate size significantly. This contrasts with Yang et al. (2023), who observed an increase in correlation length ξ for heated acid gels via USANS. The only exception in our study was found for cow rennet gels. As cow HCM rennet gel did show aggregates but did not form a continuous gel network (Fig. 4), this may explain why a clear difference in correlation length was observed for this sample. In general, the correlation length ξ is not the only parameter that determines the characteristics (including the shape and intensity) of the SESANS signal. The overall characteristics of the SESANS signal are also determined by other parameters such as the volume fraction, the building block size, the fractal dimension, and the scattering length density contrast (Andersson et al., 2008). This is illustrated in Fig. S1. It is therefore assumed that other parameters play a more predominant role in determining the changes in signal strength upon heating in the gel samples.

Additional structural information of the gels based on the fractal model can be obtained from the fractal dimension d_f and $\Delta\rho$ (Table 3). For acid gels formed from goat and cow NCM, a $d_f \approx 2.4$ was determined, while for rennet gels, a $d_f \approx 2.8$ was found. The fractal dimension for rennet gels is higher than expected, as the fractal dimension for both rennet and acid gels was previously reported to be comparable ($d_f \approx 2.3$) based on rheological experiments (Bremer et al., 1989; Zhong et al., 2004). The differences in fractal dimension d_f between acid and rennet gels indicate that these gels differ in their internal structure, indicating that in rennet gels from NCM casein micelles associate to more compact aggregates than in acid gels. The reason for this could be that, in contrast to acid gels, in rennet gels, steric repulsive forces have been removed by the cleavage of caseinomacropeptide from κ-CN, which allows the casein micelles to approach each other more closely.

When considering the effect of heat treatment an interesting behavior in the fractal dimension d_f was found. For acid gels, the fractal dimension increased to $d_f \approx 2.6$, which is in good agreement with values obtained for acid gels formed from heated and non-heated milk with USANS (Yang et al., 2023). In contrast to acid gels, the fractal dimension for HCM rennet samples decreased to $d_f \approx 2.6$ and $d_f \approx 2.7$ for cow and goat, respectively. Again, no values for rennet samples measured with SESANS have been reported earlier. These opposite effects of pre-heating of milk in the fractal dimension d_f of rennet and acid gels also translate to changes in SESANS signal strength in the same directions as changes in d_f (Fig. 3). The increase in d_f (and also building block radius) for acid gels due to heat treatment was even enough to overcompensate the decrease in both $\Delta\rho$ and ξ, resulting in a net increase of SESANS signal strength. As the density of aggregates is expected to increase for more compact aggregates, gels with a higher fractal dimension d_f are expected to show a coarser gel network on micrometer scale (Nieuwland et al., 2015, 2016). When comparing CLSM images from NCM and HCM gels (Fig. 4), NCM rennet gels indeed showed a coarser gel network with larger pores. For acid gels, the HCM gels appeared slightly more coarse than NCM gels, but differences between NCM and HCM gels were less pronounced than for rennet gels. This does not resemble the extent to which d_f changed, but still, the opposite trends in d_f align with CLSM observation. In rennet gels, the reduction in d_f may be a result of whey proteins associated with casein micelles in HCM forming an additional layer, preventing casein (partly) from aggregation and network formation. In acid gels, however, the associated whey proteins seem to help caseins to form a more compact network.

Furthermore, similar to the results on casein micelles (Table 2), a reduction in $\Delta\rho$ was observed for rennet gels formed from HCM (Table 3). This seems logical considering the increased hydration of HCM compared to NCM decreases $\Delta\rho$, and that a reduction in compactness, represented by the decrease in d_f, can lead to more entrapped water in the gel network, consequently decreasing $\Delta\rho$ (Nieuwland et al., 2016). Both phenomena are expected to decrease the SESANS signal strength. For acid gels, a slight reduction in $\Delta\rho$ was observed due to heat treatment, despite the increase in d_f, which seems

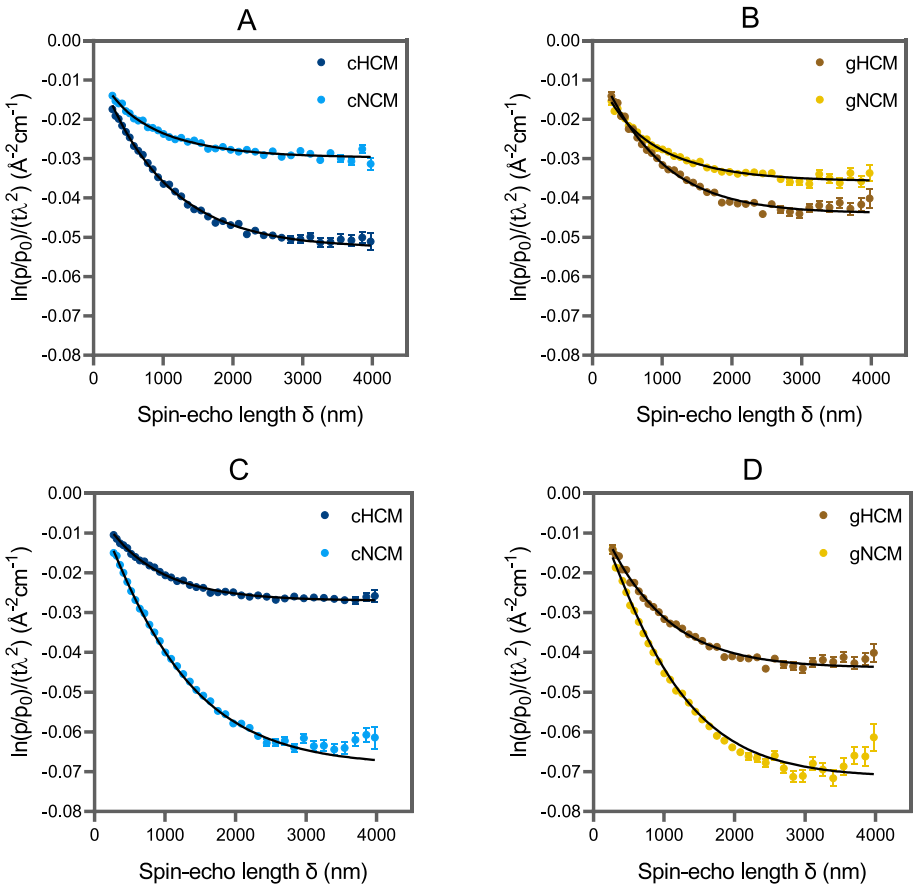

Fig. 3. SESANS signal as a function of spin-echo length (δ) for acid (A, B) and rennet (C, D) gels of cow (A, C) and goat (B, D) native (NCM) and heated (HCM) casein micelle solution. Where P and P_0 are the polarization of the neutron beams with and without passing the sample. t is the sample thickness and λ is the neutron wavelength. The solid black curves represent the fitted fractal model.

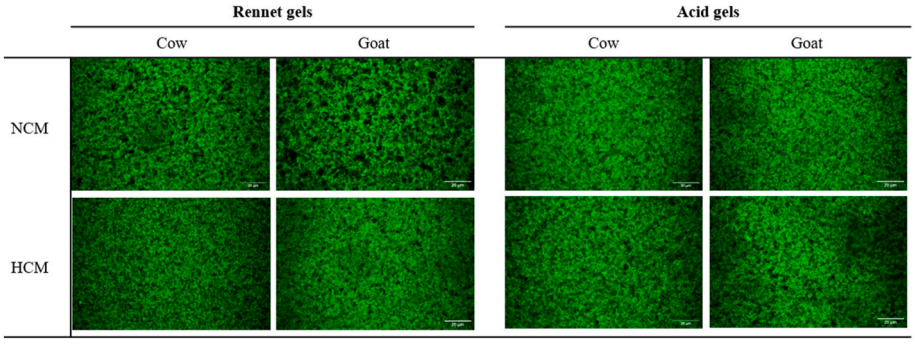

Fig. 4. CSLM images of rennet gels (6 h, 30 °C) and acid gels (14 h, 30 °C) from cow and goat native casein micelles (NCM) and heated casein micelles (HCM) incubated at 30 °C at a protein concentration of 2.6 %. Proteins are stained in green. Cow HCM was still liquid. (For interpretation of the references to colour in this figure legend, the reader is referred to the Web version of this article.)

contradictory. As the $\Delta\rho$ is expected to be influenced by changes in protein composition due to presence of whey proteins in HCM samples, but also by structural differences between the gels, the interpretation is difficult in acid gels, because both aspects would influence the overall $\Delta\rho$ in the opposite way.

3.3.3. *Relation between structural information and gel strength*

In this work, the gelation type appears to be the determining factor for the direction of the observed trends in rheological gel strength, CLSM gel coarseness, and SESANS signal strength and fractal dimension due to heat treatment. In all gel samples, the heat treatment had a significant effect on both the fractal dimension d_f (as measured by SESANS) and on the gel strength G'_{max} (Fig. 1). In the case of acid gels, an increase in d_f and a G'_{max} due to heat treatment was observed, while in the case of rennet gels heat treatment led to a decrease in d_f and G'_{max}. Therefore, one may expect that a more compact gel network (higher d_f) is linked to a stronger gel (higher G'_{max}) of the same gel type.

However, when cross-comparing the different gel types (rennet vs. acid gels) from NCM and HCM, a direct link between G'_{max} and absolute values of d_f is not straightforward. Furthermore, the milk origin (cow vs. goat milk) seems to rather influence the extent, rather than the direction *per se* upon heating. This indicates that, while the degree of structural compactness (represented by d_f) does play an important role in rheological properties of these gels, other factors, such as the nature of the

Table 3
Results obtained from describing SESANS measurements of acid and rennet gels formed from cow and goat native casein micelles (NCM) and heated casein micelles (HCM) samples as fractal networks[a].

Parameter	cNCM	cHCM	gNCM	gHCM
Median sphere radius, r[b] (nm)	39.70	44.90	72.60	92.70
Log-normal distribution parameter, σ[b]	0.30	0.30	0.30	0.30
Volume fraction, ϕ [b]	0.10	0.09	0.07	0.08
Rennet gels				
Fractal dimension, d_f [c]	2.80 ± 0.01	2.57 ± 0.04	2.89 ± 0.02	2.71 ± 0.04
Correlation length, ξ [c] (nm)	902.29 ± 32.51	770.34 ± 61.81	757.03 ± 29.46	747.22 ± 48.71
SLD difference, Δρ[c] (10^{-6} Å^{-2})	0.77 ± 0.01	0.66 ± 0.01	0.87 ± 0.01	0.71 ± 0.00
Reduced χ-square, χ^2_R	1.30	0.52	1.22	1.47
Acid gels				
Fractal dimension, d_f [c]	2.36 ± 0.03	2.63 ± 0.02	2.38 ± 0.05	2.62 ± 0.04
Correlation length, ξ [c](nm)	977.65 ± 101.22	902.31 ± 43.39	954.73 ± 109.44	771.62 ± 56.25
SLD difference, Δρ[c] (10^{-6} Å^{-2})	0.83 ± 0.01	0.79 ± 0.01	0.83 ± 0.01	0.75 ± 0.00
Reduced χ-square, χ^2_R	1.09	1.10	0.71	1.09

[a] Parameters are reported as mean ± standard deviation.
[b] Fixed parameter.
[c] Fitted parameter.

building blocks and how they interact, are also critical. Indeed, Mellema et al. (2002) previously pointed out that one cannot simply use fractal dimension alone to establish a clear connection between structure and rheological properties of gels. Furthermore, it has to noted, that acid- and rennet-induced gelation have a significantly different gelation mechanism.

When comparing rennet gel samples, for both goat NCM and HCM, higher maximum gel strength (G'_{max}) values as well as higher d_f values were obtained compared to the corresponding cow sample. It is therefore hypothesized that one contributing factor for goat milk rennet gels to form stronger gels is that goat casein micelles seem to aggregate to more compact gel structures than cow casein micelles.

Acid gels, on the other hand presented noticeable changes in d_f due to heat treatment, but no significant changes in d_f between cow and goat samples were seen for acid gels, despite clear difference between in G'_{max} of cow and goat HCM acid gels. Therefore, d_f alone was unable to explain the large differences in G'_{max} between acid gels from goat and cow samples. This reinforces our previous discussion that, besides fractal dimension, other factors must be considered.

Previous research indicated that casein micelles maintain their micellar structure during acid gelation to a large extent, also after the micellar calcium phosphate has been dissolved. However, it was also shown that casein micelles get partly liberated and thus dissociate during acidification and that intramicellar rearrangements occur upon acidification (Dalgleish & Law, 1988; Horne, 1999; Moitzi et al., 2010). These dissociated caseins are more mobile and could result in a more interconnected casein network than in rennet gels. Furthermore, HCM acid gels, it is believed that the increased gel strength compared to NCM acid gels is caused by additional connections due to denatured and associated whey proteins helping to bridge casein micelles (Lucey et al., 1997; Mottar et al., 1989). Our previous research has shown that cow and goat milk respond quite differently to heat treatment and that this may be translated into different roles or extents of participation of denatured whey protein in the gel network (Breunig, Fan, et al., 2025). Hence, a fractal model of spherical particles may not be able to fully describe these gels, especially HCM gels, appropriately. A model of particle gel featuring elements of polymer gels could perhaps better describe such gels. However, to our knowledge, no suitable model is available to probe such a mixed structure.

Nevertheless, by applying the fractal model to the SESANS data, we could obtain satisfactory fits to the experimental data, which provided quantitative parameters that can expand our understanding of heat-induced structural changes in both rennet and acid gels between cow and goat milk and how those could be linked to changes in gel strength. However, it has to be acknowledged that this model has its limitations to be able to fully describe the system to the point of predicting its rheological properties, especially for acid gels. The exact relationship between gel strength and structural information is not yet conclusive in this study, but it may be clarified in the future by applying different appropriate models to different types of gels.

Nevertheless, the changes in SESANS signal strength due to heat treatment for acid gels were more pronounced for cow milk when compared to goat milk. Likewise, gel strength (Fig. 1) of cow milk samples was more affected by heat treatment than goat milk gels. In rennet gels, opposite trends in the change of SESANS signal strength were observed, but similar to acid gels, both the gel strength and the signal strength were more affected for cow milk gels upon heating. It is therefore reasonable to hypothesize that cow milk gels (both acid- and rennet-induced) undergo more significant structural modifications due to heat treatment than their goat counterparts.

It is proposed that heat-induced structural changes in the casein micelles could be connected to changes in the gel network. Heat treatment-induced changes in size and hydration of micelles alone (Table 2) are not able to explain the different changes in gel structure, as examined in this study. However, heat-induced changes of casein micelles due to whey protein denaturation and aggregation onto the casein micelle surface could have altered the way casein micelles interact to form a network, which appears to be different in cow and goat milk. Even though it is unknown how changes on the casein micelle surface compare in goat and cow milk upon heat treatment, previous SANS experiments, which probe the structure of casein micelles on smaller length scales, indicated that heat-induced changes are noticeably more accentuated for cow casein micelles than for goat casein micelles (Breunig, Fan, et al., 2025).

4. Conclusion

Casein micelles, as well as rennet and acid-induced casein gels of unheated and heated goat and cow milk, were compared. A novel combination of rheology, CLSM, DLS, and SESANS was employed to allow a more thorough investigation. It was shown that SESANS can be a valuable tool to probe changes in properties of casein micelles, such as size and hydration, between different milk sources and after heat treatment. By modeling micelles as sticky hard spheres, goat casein micelles were found to be generally larger and less hydrated than the cow casein micelles. SESANS data of milk gels prepared with and without heat treatment were described using a fractal model. Preheating of milk showed opposite effects on changes in the fractal dimension and SESANS signal strength in acid and rennet gels. Opposite effects were also observed for gel strength and homogeneity in these two types of gels due to heat treatment. Together, this finding indicates that the type of gelation (rennet or acid) drives the direction of changes in gel compactness (fractal dimension), gel strength, gel coarseness, and SESANS signal strength. The origin of the milk (cow or goat) has an important effect on the extent (rather than the direction itself) of these observed changes. The use of the fractal model could provide good fits to the experimental SESANS data and allowed the estimation of structural parameters that are correlated to changes in gel strength and coarseness during heat treatment. Nevertheless, the structural parameters estimated with the fractal model were not able to explain, for example, the large differences in gel strength between cow and goat acid gels. This

may be due to additional, unaccounted factors arising due to the chemical transformations during gelation and heat treatment, including denaturation of whey protein and modifications of the internal organization of micelles, as well as their surfaces. Still, the SESANS data indicates that cow milk gels are much more susceptible to heat-induced changes than goat milk gels, which may be linked to more significant changes in the internal micellar structure of cow casein micelles when compared to goat micelles. This emphasizes the importance of taking a closer look at the structure and colloidal properties of the casein micelles as critical building blocks in the development of milk-based gels and paves the way towards the exploration of more complex models to describe such gels. In addition, we hope that this study provides inspiration for further advances in the usage of SESANS and other scattering methods in the study and characterization of food materials.

CRediT authorship contribution statement

Swantje Breunig: Writing – review & editing, Writing – original draft, Visualization, Methodology, Formal analysis, Conceptualization. **Zekun Fan:** Writing – review & editing, Visualization, Methodology, Formal analysis, Conceptualization. **Renske Bouma:** Writing – review & editing, Methodology, Conceptualization. **Gregory N. Smith:** Writing – review & editing, Methodology. **Rafael V.M. Freire:** Writing – review & editing, Conceptualization. **Ilja K. Voets:** Writing – review & editing, Conceptualization. **Steven R. Parnell:** Writing – review & editing, Methodology. **Kasper Hettinga:** Writing – review & editing, Supervision, Conceptualization. **Etske Bijl:** Writing – review & editing, Supervision, Project administration, Conceptualization.

Declaration of competing interest

The authors declare that they have no known competing financial interests or personal relationships that could have appeared to influence the work reported in this paper.

Acknowledgements

This publication was financially supported by the Ausnutria B.V. (Zwolle, the Netherlands) and the 'Animal-free milk proteins' project (with project number NWA.1292.19.302) of the NWA research program 'Research along Routes by Consortia (ORC)', which is funded by the Dutch Research Council (NWO). We acknowledge ISIS Neutron and Muon Source for beamtime on Larmor. Data is available here: 10.5286/ISIS.E.RB2469000. This work was also financially supported by China Scholarship Council (project number: 202007720061). The authors thank the farmers of the cow and goat herds for providing the milk. This work benefited from the use of the SasView application, originally developed under NSF award DMR-0520547. SasView contains code developed with funding from the European Union's Horizon 2020 research and innovation program under the SINE2020 project, grant agreement No 654000.

Appendix A. Supplementary data

Supplementary data to this article can be found online at https://doi.org/10.1016/j.foodhyd.2025.112242.

Data availability

Data will be made available on request.

References

Akshit, F. N. U., Deshwal, G. K., Sharma, H., Kumar, P., Maddipatla, D. K., Singh, M. P., & Goksen, G. (2024). Technological challenges in production of goat milk products and strategies to overcome them: A review. *International Journal of Food Science and Technology, 59*(1), 6–16. https://doi.org/10.1111/IJFS.16782

Andersson, R., Van Heijkamp, L. F., De Schepper, I. M., & Bouwman, W. G. (2008). Analysis of spin-echo small-angle neutron scattering measurements. *Journal of Applied Crystallography, 41*(5), 868–885. https://doi.org/10.1107/S0021889808026770

Arnold, O., Bilheux, J. C., Borreguero, J. M., Buts, A., Campbell, S. I., Chapon, L., Doucet, M., Draper, N., Ferraz Leal, R., Gigg, M. A., Lynch, V. E., Markvardsen, A., Mikkelson, D. J., Mikkelson, R. L., Miller, R., Palmen, K., Parker, P., Passos, G., Perring, T. G., … Zikovsky, J. (2014). Mantid—Data analysis and visualization package for neutron scattering and μ SR experiments. *Nuclear Instruments and Methods in Physics Research Section A: Accelerators, Spectrometers, Detectors and Associated Equipment, 764*, 156–166. https://doi.org/10.1016/J.NIMA.2014.07.029

Bakker, J. H., Washington, A. L., Parnell, S. R., Van Well, A. A., Pappas, C., & Bouwman, W. G. (2020). Analysis of SESANS data by numerical Hankel transform implementation in SasView. *Journal of Neutron Research, 22*(1), 57–70. https://doi.org/10.3233/JNR-200154

Baxter, R. J. (1968). Percus-Yevick equation for hard spheres with surface adhesion. *The Journal of Chemical Physics, 49*(6), 2770–2774. https://doi.org/10.1063/1.1670482

Bijl, E., De Vries, R., Van Valenberg, H., Huppertz, T., & Van Hoojdonk, T. (2014). Factors influencing casein micelle size in milk of individual cows: Genetic variants and glycosylation of κ-casein. *International Dairy Journal, 34*(1), 135–141. https://doi.org/10.1016/j.idairyj.2013.08.001

Bonfatti, V., Grigoletto, L., Cecchinato, A., Gallo, L., & Carnier, P. (2008). Validation of a new reversed-phase high-performance liquid chromatography method for separation and quantification of bovine milk protein genetic variants. *Journal of Chromatography A, 1195*(1–2), 101–106. https://doi.org/10.1016/j.chroma.2008.04.075

Bouma, R., Bijl, E., Thiel, A., & Hettinga, K. (2025). Comparing coagulation behaviour of reassembled and native casein micelles during renneting, acid gelation and gastric clotting. *Food Hydrocolloids, 168*, Article 111441. https://doi.org/10.1016/J.FOODHYD.2025.111441

Bouwman, W. G. (2021). Spin-echo small-angle neutron scattering for multiscale structure analysis of food materials. *Food Structure, 30*, Article 100235. https://doi.org/10.1016/J.FOOSTR.2021.100235

Bouwman, W. G., Krouglov, T. V., Plomp, J., Grigoriev, S. V., Kraan, W. H., & Rekveldt, M. T. (2004). SESANS studies of colloid phase transitions, dairy products and polymer fibres. *Physica B: Condensed Matter, 350*(4), 140–146. https://doi.org/10.1016/j.physb.2004.04.013

Bremer, L. G. B., Van Vliet, T., & Walstra, P. (1989). Theoretical and experimental study of the fractal nature of the structure of casein gels. *Journal of the Chemical Society, Faraday Transactions 1: Physical Chemistry in Condensed Phases, 85*(10), 3359–3372. https://doi.org/10.1039/F19898503359

Breunig, S., Crooijmans, R. P. M. A., Bovenhuis, H., Hettinga, K., & Bijl, E. (2024). Linking variation in the casein fraction and salt composition to casein micelle size in milk of Dutch dairy goats. *Journal of Dairy Science, 107*(9), 6474–6486. https://doi.org/10.3168/jds.2023-24548

Breunig, S., Fan, Z., Keijzer, P., Hettinga, K., & Bijl, E. (2025). Heating affects gelation properties and casein micelle structure in goat and cow milk differently. *Food Structure.* , Article 100438. https://doi.org/10.1016/J.FOOSTR.2025.100438

Breunig, S., Gonzalez-Prendes, R., Crooijmans, R. P. M. A., Hettinga, K., Bovenhuis, H., & Bijl, E. (2025). Liquid chromatography-MS–based identification of casein variants in Dutch goat milk and their effect on casein composition, protein content, and micelle size. *Journal of Dairy Science, 108*(4), 3258–3272. https://doi.org/10.3168/JDS.2024-25823

Callaghan-Patrachar, N., Peyronel, F., Pink, D. A., Marangoni, A. G., & Adams, C. P. (2021). USANS and SANS investigations on the coagulation of commercial bovine milk: Microstructures induced by calf and fungal rennet. *Food Hydrocolloids, 116*, Article 106622. https://doi.org/10.1016/J.FOODHYD.2021.106622

Dalgleish, D. G., & Law, A. J. R. (1988). pH-Induced dissociation of bovine casein micelles. I. Analysis of liberated caseins. *Journal of Dairy Research, 55*(4), 529–538. https://doi.org/10.1017/S0022029900033306

de Asís Ruiz Morales, F., Genís, J. M. C., & Guerrero, Y. M. (2019). Current status, challenges and the way forward for dairy goat production in Europe. *Asian-Australasian Journal of Animal Sciences, 32*(8 Suppl), 1256–1265. https://doi.org/10.5713/AJAS.19.0327

Donato, L., & Guyomarc'h, F. (2009). Formation and properties of the whey protein/κ-casein complexes in heated skim milk - A review. *Dairy Science & Technology, 89*(1), 3–29. https://doi.org/10.1051/dst:2008033

Fan, Z., Fehér, B., Hettinga, K., Voets, I. K., & Bijl, E. (2024). Effect of temperature, pH and calcium phosphate concentration on the properties of reassembled casein micelles. *Food Hydrocolloids, 149*, Article 109592. https://doi.org/10.1016/j.foodhyd.2023.109592

Gaucher, I., Boubellouta, T., Beaucher, E., Piot, M., Gaucheron, F., & Dufour, E. (2008). Investigation of the effects of season, milking region, sterilisation process and storage conditions on milk and UHT milk physico-chemical characteristics: A multidimensional statistical approach. *Dairy Science & Technology, 88*, 291–312. https://doi.org/10.1051/dst:2007022

Gilbert, E. P. (2019). Small-angle X-Ray and neutron scattering in food colloids. *Current Opinion in Colloid & Interface Science, 42*, 55–72. https://doi.org/10.1016/J.COCIS.2019.03.005

Horne, D. S. (1999). Formation and structure of acidified milk gels. *International Dairy Journal, 9*(3–6), 261–268. https://doi.org/10.1016/S0958-6946(99)00072-2

Horne, D. S. (2020). Casein micelle structure and stability. In M. Boland, & S. Harjinder (Eds.), *Milk proteins: From expression to food* (3rd ed., pp. 213–250). Academic Press. https://doi.org/10.1016/B978-0-12-815251-5.00006-2.

Ingham, B., Smialowska, A., Kirby, N. M., Wang, C., & Carr, A. J. (2018). A structural comparison of casein micelles in cow, goat and sheep milk using X-ray scattering. *Soft Matter, 14*(17), 3336–3343. https://doi.org/10.1039/c8sm00458g

Jacob, M., Nöbel, S., Jaros, D., & Rohm, H. (2011). Physical properties of acid milk gels: Acidification rate significantly interacts with cross-linking and heat treatment of milk. *Food Hydrocolloids, 25*(5), 928–934. https://doi.org/10.1016/J.FOODHYD.2010.09.003

Jenness, R., & Koops, J. (1962). Preparation and properties of salt solution which simulates milk ultrafiltrate. *Nederlands Melk- en Zuiveltijdschrift, 16*(3), 153–164.

Kotlarchyk, M., & Chen, S. H. (1983). Analysis of small angle neutron scattering spectra from polydisperse interacting colloids. *The Journal of Chemical Physics, 79*(5), 2461–2469. https://doi.org/10.1063/1.446055

Li, R., Christine Jæger, T., Rovers, T. A. M., Svensson, B., Ipsen, R., Kirkensgaard, J. J. K., & Bygvrå Hougaard, A. (2022). In situ SAXS study of non-fat milk model systems during heat treatment and acidification. *Food Research International, 157*, Article 111292. https://doi.org/10.1016/j.foodres.2022.111292

Li, S., Delger, M., Dave, A., Singh, H., & Ye, A. (2023). Acid and rennet gelation properties of sheep, goat, and cow milks: Effects of processing and seasonal variation. *Journal of Dairy Science, 106*, 1611–1625. https://doi.org/10.3168/jds.2022-22561

Li, F., Parnell, S. R., Dalgliesh, R., Washington, A., Plomp, J., & Pynn, R. (2019). Data correction of intensity modulated small angle scattering. *Scientific Reports, 9*(1), 1–8. https://doi.org/10.1038/s41598-019-44493-9, 2019 9:1.

Lucey, J. A. (2020). Milk protein gels. In M. Boland, & H. Singh (Eds.), *Milk proteins: From expression to food* (3rd ed., pp. 599–632). Academic Press. https://doi.org/10.1016/B978-0-12-815251-5.00016-5.

Lucey, J. A., & Singh, H. (1998). Formation and physical properties of acid milk gels: A review. *Food Research Iniernational, 30*(7), 529–542. https://doi.org/10.1016/S0963-9969(98)00015-5

Lucey, J. A., Tamehana, M., Singh, H., & Munro, P. A. (1998). Effect of interactions between denatured whey proteins and casein micelles on the formation and rheological properties of acid skim milk gels. *Journal of Dairy Research, 65*(4), 555–567. https://doi.org/10.1017/S0022029998003057

Lucey, J. A., Tet Teo, C., Munro, P. A., & Singh, H. (1997). Rheological properties at small (dynamic) and large (yield) deformations of acid gels made from heated milk. *Journal of Dairy Research, 64*, 591–600. https://doi.org/10.1017/S0022029997002380

Mellema, M., Walstra, P., van Opheusden, J. H. J., & van Vliet, T. (2002). Effects of structural rearrangements on the rheology of rennet-induced casein pArticle gels. *Advances in Colloid and Interface Science, 98*(1), 25–50. https://doi.org/10.1016/S0001-8686(01)00089-6

Miller, B. A., & Lu, C. D. (2019). Current status of global dairy goat production: An overview. *Asian-Australasian Journal of Animal Sciences, 32*(8), 1219–1232. https://doi.org/10.5713/ajas.19.0253

Moitzi, C., Menzel, A., Schurtenberger, P., & Stradner, A. (2010). The pH induced sol-gel transition in skim milk revisited. A detailed study using time-resolved light and X-ray scattering experiments. *Langmuir, 27*(6), 2195–2203. https://doi.org/10.1021/la102488g

Mottar, J., Bassier, A., Joniau, M., & Baert, J. (1989). Effect of heat-induced Association of Whey proteins and casein micelles on yoghurt texture. *Journal of Dairy Science, 72*(9), 2247–2256. https://doi.org/10.3168/JDS.S0022-0302(89)79355-3

Nieuwland, M., Bouwman, W. G., Bennink, M. L., Silletti, E., & de Jongh, H. H. J. (2015). Characterizing length scales that determine the mechanical behavior of gels from crosslinked casein micelles. *Food Biophysics, 10*(4), 416–427. https://doi.org/10.1007/S11483-015-9399-Y/FIGURES/9

Nieuwland, M., Bouwman, W. G., Pouvreau, L., Martin, A. H., & de Jongh, H. H. J. (2016). Relating water holding of ovalbumin gels to aggregate structure. *Food Hydrocolloids, 52*, 87–94. https://doi.org/10.1016/J.FOODHYD.2015.06.018

Park, Y. W. (2017). Goat milk-chemistry and nutrition. In Y. W. Park, G. F. W. Haenlein, & W. L. Wendorff (Eds.), *Handbook of milk of non-bovine mammals* (2nd ed., pp. 42–83). John Wiley & Sons, Ltd. Second Edition.

Rekveldt, M. T. (1996). Novel SANS instrument using neutron spin echo. *Nuclear Instruments and Methods in Physics Research B, 114*, 366–370. https://doi.org/10.1016/0168-583X(96)00213-3

Remeuf, F., & Lenoir, J. (1986). Relationship between the physico-chemical characteristics of goat's milk and its rennetability. *Bulletin International Dairy Federation, 202*, 68–72. https://doi.org/10.5040/9781472597199.ch-001

Roy, D., Ye, A., Moughan, P. J., & Singh, H. (2020). Gelation of milks of different species (dairy cattle, goat, sheep, red deer, and water buffalo) using glucono-δ-lactone and pepsin. *Journal of Dairy Science, 103*, 5844–5862. https://doi.org/10.3168/jds.2019-17571

Smith, G. N. (2021). Revisiting neutron scattering data from deuterated milk. *Food Hydrocolloids, 113*, Article 106511. https://doi.org/10.1016/j.foodhyd.2020.106511

Smith, G. N., Brok, E., Christiansen, M. V., & Ahrné, L. (2020). Casein micelles in milk as sticky spheres. *Soft Matter, 16*, Article 9955. https://doi.org/10.1039/d0sm01327g

Teixeira, J. (1998). Small-angle scattering by fractal systems. *Journal of Applied Crystallography, 21*(6), 781–785. https://doi.org/10.1107/S0021889888000263

Tromp, R. H., & Bouwman, W. G. (2007). A novel application of neutron scattering on dairy products. *Food Hydrocolloids, 21*(2), 154–158. https://doi.org/10.1016/J.FOODHYD.2006.02.008

Van Heijkamp, L. F., De Schepper, I. M., Strobl, M., Hans Tromp, R., Heringa, J. R., & Bouwman, W. G. (2010). Milk gelation studied with small angle neutron scattering techniques and monte carlo simulations. *Journal of Physical Chemistry A, 114*(7), 2412–2426. https://doi.org/10.1021/jp9067735

Yang, Z., Cheng, L., De Campo, L., Gilbert, E. P., Mittelbach, R., Luo, L., Ye, A., Li, S., & Hemar, Y. (2023). Microstructural evolution during acid induced gelation of cow, goat, and sheep milk probed by time-resolved (Ultra)-small angle neutron scattering. *Food Hydrocolloids, 137*, Article 108381. https://doi.org/10.1016/j.foodhyd.2022.108381

Zhong, Q., Daubert, C. R., & Velev, O. D. (2004). Cooling effects on a model rennet casein gel system: Part I. Rheological characterization. *Langmuir, 20*(18), 7399–7405. https://doi.org/10.1021/la036147w